

Supplementary Information

Oxide-Oxide Nanojunctions in coaxial SnO₂/TiO₂, SnO₂/V₂O₃ and SnO₂/(Ti_{0.5}V_{0.5})₂O₃ Nanowire Heterostructures

Reza Zamani,^{a,b} Raquel Fiz,^c Jun Pan,^c Thomas Fischer,^c Sanjay Mathur,^{*c} Joan Ramon Morante^{*b,d} and Jordi Arbiol ^{*a,e}

^a Institut de Ciència de Materials de Barcelona, ICMAB-CSIC, E-08193 Bellaterra, CAT, Spain; E-mail: arbiol@icrea.cat

^b Catalonia Institute for Energy Research (IREC), E-08930 Sant Adrià del Besòs, CAT, Spain; E-mail: jrmorante@irec.cat

^c Institute of Inorganic Chemistry, University of Cologne, Cologne, Germany; E-mail: sanjay.mathur@uni-koeln.de

^d Departament d'Electrònica, Universitat de Barcelona, E-08028 Barcelona, CAT, Spain

^e Institució Catalana de Recerca i Estudis Avançats (ICREA), E-08010 Barcelona, CAT, Spain

CONTENTS Page

S1. Atomic simulation of the interfaces between rutile SnO ₂ NW core and different shells: (a) Ti ₂ O, (b) Ti ₂ O ₃ , (c) TiO ₂ rutile and (d) TiO ₂ anatase. (Figure S1)	2
S2. Formation mechanism of SnO ₂ - based heterostructures. (Figure S2)	2
S3. In-situ mass spectrometrical analysis of the gas phase during the deposition process. (Figure S3)	3

S1. Atomic simulation of the interfaces between rutile SnO₂ NW core and different shells: (a) Ti₂O, (b) Ti₂O₃, (c) TiO₂ rutile and (d) TiO₂ anatase.

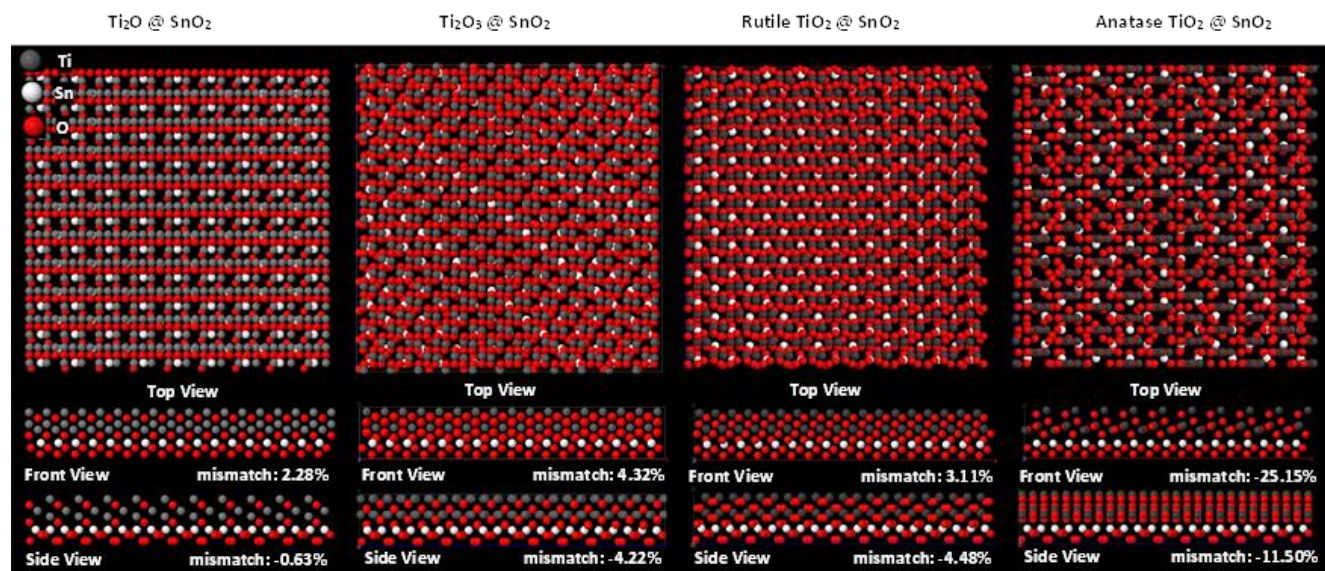


Figure S1. Atomic simulation of the interfaces between rutile SnO₂ NW core and different shells: (a) Ti₂O, (b) Ti₂O₃, (c) TiO₂ rutile and (d) TiO₂ anatase. Top views show the $[10-10]_{\text{Ti}2\text{O}} // [0-11]_{\text{SnO}2}$ in the case of Ti₂O on SnO₂, $[11-20]_{\text{Ti}2\text{O}3} // [0-11]_{\text{SnO}2}$ zone axis in the case of Ti₂O₃ on SnO₂ and $[0-11]_{\text{TiO}2} // [0-11]_{\text{SnO}2}$ in the case of TiO₂ rutile and anatase on SnO₂. Front views are visualized along the $[0001]_{\text{Ti}2\text{O}/\text{Ti}2\text{O}3} // [100]_{\text{SnO}2}$ zone axis in the case of Ti₂O and Ti₂O₃ on SnO₂, and along the $[100]_{\text{TiO}2} // [100]_{\text{SnO}2}$ zone axis in the case of TiO₂ rutile and anatase on SnO₂. Finally, the side view corresponds to the $[-12-10]_{\text{Ti}2\text{O}} // [011]_{\text{SnO}2}$, $[-1100]_{\text{Ti}2\text{O}3} // [011]_{\text{SnO}2}$ and $[011]_{\text{TiO}2 \text{ anat/rutile}} // [011]_{\text{SnO}2}$ directions. In each case mismatch percentage is indicated under the model.

S2. Formation mechanism of SnO₂- based heterostructures.

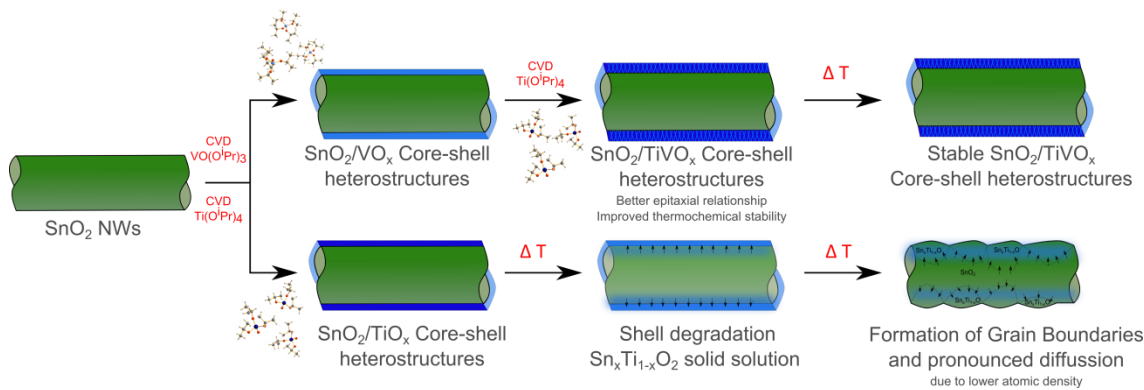


Figure S2. Formation mechanism of SnO₂- based heterostructures. While titania shells degrade, vanadia overlayers show improved epitaxial relationships and thermochemical stability.

S3. In-situ mass spectrometrical analysis of the gas phase during the deposition process.

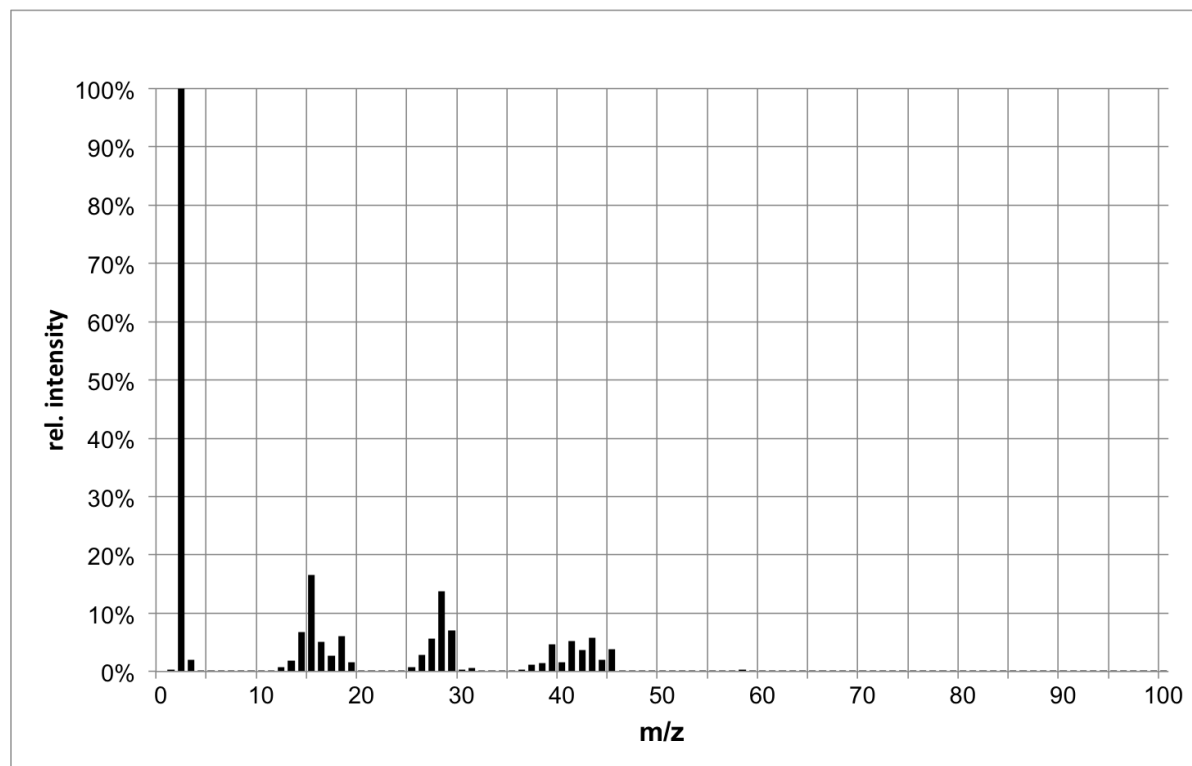


Figure S3. *In-situ* mass spectrometrical analysis of the gas phase during the deposition process of $\text{Ti}(\text{OPr})_4$: $m/z=2$ (H_2^+), 18 (H_2O^+), 15 (CH_3^+), 42 (C_3H_5^+), 45 ($\text{C}_2\text{H}_6\text{O}^+$), 59 ($\text{C}_3\text{H}_7\text{O}^+$).